Desalination and Water Treatment
www.deswater.com
doi: 10.5004/dwt.2023.29397

288 (2023) 223–233
March

Kinetics of changes in chemical oxygen demand values in leachate treated with Fenton reagent

Joanna Muszyńska, Jarosław Gawdzik*

Faculty of Environmental, Geomatic and Energy Engineering, Kielce University of Technology, al. Tysiąclecia Państwa Polskiego 7, 25-314 Kielce, Poland, Tel.: +48-41-34-24-571; emails: jdlugosz@tu.kielce.pl (J. Muszyńska), jgawdzik@tu.kielce.pl (J. Gawdzik)

Received 4 October 2022; Accepted 7 February 2023

ABSTRACT

In this study, a new second-order reaction kinetics model was developed for the elimination of chemical oxygen demand (COD) in landfill leachate treatment with Fenton reagent. The objective of the reaction was to reduce COD, UVA(254) and color in the process of landfill leachate treatment with Fenton reagent. The model was verified on sample data obtained experimentally. Oxidation concerns landfill leachate organic pollutants in the presence of Fe(II) for different oxidant and catalyst concentrations. The results of experiments demonstrated that the use of Fenton reaction have brought the expected outturns. As a result of using the Fenton reaction, the content of COD was lowered from 1.742 to 0.177 g·L^{-1}. On the basis of the investigations, the values of the reaction rate constants k_2 were estimated from 0.0018 to 0.0023 L·g^{-1}·min^{-1}. It was shown that the conversion degree can become a useful tool for the assessment of the oxidation reaction kinetics.

Keywords: Advanced oxidation processes; Chemical oxygen demand; Reaction kinetics; Landfill leachate; Reaction rate

1. Introduction

Currently, sustainable use of natural resources has become a top priority. In the Waste Framework Directive, it is declared that waste management must be regulated by the '4Rs principle'. As a result, the so-called 'hierarchy of recovery', including Reduction, Reuse, Recycling, and Recovery, wase stablished so that waste and energy could be used in a rational manner [1]. However, the oldest method of landfilling is still the most widely applied waste management strategy (in 2014, 31% of waste in the EU was disposed of by landfilling) [2,3]. The operation of the landfill, and also physical, chemical and biological phenomena that occur in it, lead to environmental hazards. They result from, among others, landfill gas emissions, pathogens, odours, noise, pests and the production of highly contaminated leachate [2,4–6]. Even if landfills are constructed in accordance with current legislation, they still have a negative impact on the environment, for example, through the spread of bioaerosol after the facility has been closed and land reclaimed [2,6]. It can be observed that after the waste deposition in the landfill, a delay in leachate release can take half a year or longer. Leachate formation can also occur immediately after the waste is deposited in the landfill if the bedrock porosity is very high. Typically, large amounts of leachate are produced 1–2 y after waste deposition. Heavy precipitation events also result in increased leachate production [7,8].

The choice of leachate treatment technology is a complex process which depends on a number of determinants. They include changes in leachate quantity and quality, the necessity to minimise leachate treatment costs (chemicals purchase, operation and maintenance of the facility, energy, utilities). Conventional leachate treatment methods are not always effective or technologically viable, especially for the removal of substances that are non-biodegradable pollution. As a result, the application of advanced oxidation processes (AOPs) comes as an alternative to conventional methods [9–11].

* Corresponding author.

Presented at the 15th Scientific Conference on Micropollutants in the Human Environment, 14–16 September 2022, Częstochowa, Poland

Leachate treatment based on the Fenton method offers high efficiency of contaminant reduction. The main disadvantages of this process lie in a high demand for reagents and large production of sludge, which, however, can be appropriately managed (coagulant preparation, adsorbent, iron source, fertilizer, heterogeneous Fenton catalyst, a sludge conditioning agent),or reduced due to the optimised reagent dosage [3,9,12]. The classical Fenton process involves a series of chemical reactions which, together with the reaction rates k, are illustrated by Eqs. (1)–(9) shown in Table 1 [13,14]. The Fenton process is based on the reaction (at optimum pH) of Fe^{2+} ions and H_2O_2 to produce hydroxyl radicals ($^{\bullet}OH$). In addition to hydroxyl radicals, hydroperoxyl/superoxide radicals ($^{\bullet}O_2H$) are also obtained in a series of reactions in the process. They can also remove contaminants, however, that happens far more slowly than it is the case with $^{\bullet}OH$ [15–17].

The complexity of the Fenton process and the composition of landfill leachate (high content of dissolved organic matter and inorganic ions) make it difficult to apply conventional kinetic method to describe the landfill leachate degradation reaction. In accordance with Wu et al. [18], the Fenton process should be divided into two stages: stage I involves the consumption of the most of H_2O_2 and Fe^{2+} and the formation of the most of the $^{\bullet}OH$. Stage II covers a series of Fenton-like reactions. It is only this approach to the Fenton process that allows the development of kinetic models to optimise the Fenton reaction in leachate treatment. Based on investigations into the kinetics of Fenton reaction at 15°C to 30°C, Aygun et al. [14] found that the temperature increase advantageously contributes to chemical oxygen demand (COD) removal and sludge dewatering. After only 30 min at 25°C, 55.7% of COD was removed (the initial COD was 3.82×10^4 mg·L^{-1}). The authors described overall reaction kinetics using a second-order rate equation followed by zero-order equation at the apparent kinetic constants at 30°C for $k_2 = 3.16 \times 10^{-3}$ and $k_0 = 0.171$ g·L^{-1}·min^{-1}. Ahmadian et al. [19] expressed Fenton kinetics with respect to COD, total suspended solids, total organic carbon (TOC) and color removal using zero-order, first-order and pseudo-second-order kinetic equations shown in Table 2.

As regards the Fenton process, parameters relevant for the outcome of the treatment include the following:

- pH value – the recommended pH range is 2–5. However, Zhang et al. [20] reported the best leachate treatment results were obtained in a narrow range of 2–3. It should be noted that Singh and Tang [21] found the optimum pH for the Fenton process in raw and coagulated leachates ranged 2.5–4.5 (median 3.0). The results were based on the statistical analysis of the optimum operating conditions described in the peer-reviewed publications.
- dosage and H_2O_2/Fe^{2+} ratio, too high ratio of H_2O_2 relative to the substrate can result in the binding of $^{\bullet}OH$s by

Table 1
Chemical reactions in the Fenton process and the reaction rates *k* [13,14]

Reaction No.	Reactions	Reaction rate *k* (L·mol^{-1}·s^{-1})	Rate constant (m^{-1}·s^{-1})
1	$H_2O_2 + Fe^{2+} \rightarrow Fe^{3+} + {}^{\bullet}OH + OH^-$	$(0.4–0.8) \times 10^2$	41.70
2	$H_2O_2 + Fe^{3+} \rightarrow Fe^{2+} + {}^{\bullet}O_2H + H^+$	9.1×10^{-7}	2.0×10^{-3}
3	$Fe^{2+} + {}^{\bullet}OH \rightarrow Fe^{3+} + OH$	$(2.5–5.0) \times 10^8$	3.3×10^7
4	$Fe^{2+} + {}^{\bullet}O_2H \rightarrow Fe^{3+} + HO_2^-$	$(0.7–1.5) \times 10^6$	7.8×10^5
5	$Fe^{3+} + {}^{\bullet}O_2H \rightarrow Fe^{2+} + O_2 + H^+$	$(0.3–2.1) \times 10^6$	3.2×10^8
6	$^{\bullet}OH + {}^{\bullet}OH \rightarrow H_2O_2$	$(5–8) \times 10^9$	1.3×10^6
7	$^{\bullet}OH + H_2O_2 \rightarrow {}^{\bullet}O_2H + H_2O$	$(1.7–4.5) \times 10^7$	2.3×10^6
8	$^{\bullet}O_2H + {}^{\bullet}O_2H \rightarrow H_2O_2 + O_2$	$(0.8–2.2) \times 10^6$	7.1×10^9
9	$^{\bullet}OH + {}^{\bullet}O_2H \rightarrow H_2O + O_2$	1.4×10^6	5.2×10^9

Table 2
Equations, linear forms and results of the kinetics model acc. [19]

Kinetic model	Equation	Linear form	Parameter	Chemical oxygen demand	Total organic carbon	Total suspended solids	Color
Zero-order	$r_c = \frac{dC}{dt} = k_0$	$C–C_0 = –k_0t$	k_0	27.93	4.48	9.04	18.58
			R^2	0.93	0.88	0.94	0.76
First-order	$r_c = \frac{dC}{dt} = k_1C$	$\ln\frac{C}{C_0} = –k_1t$	k_1	0.012	0.004	0.009	0.013
			R^2	0.98	0.92	0.99	0.91
Second-order	$r_c = \frac{dC}{dt} = k_2C^2$	$\frac{1}{C} – \frac{1}{C_0} = k_2t$	k_2	6×10^{-6}	4×10^{-6}	1×10^{-5}	1×10^{-5}
			R^2	0.97	0.91	0.95	0.94

where r_c is the rate of conversion, k_0, k_1, k_2 are reaction rate coefficients, t is time, and C_0 and C are the initial and final concentrations of the constituent in the liquid, respectively.

H_2O_2. Additionally, H_2O_2 is harmful to many organisms, which is of particular relevance for mixed processes. In those methods, the Fenton reaction precedes biological processes. Furthermore, too high ratio of H_2O_2 makes the determined COD value to be overestimated. Conversely, excessive Fe^{2+} ratio leads to an increase in dissolved solids in the treated landfill leachate [13,16,22,23]. According to Singh and Tang [21], the optimum H_2O_2/Fe^{2+} weight ratio is 1.8, whereas H_2O_2/COD and Fe^{2+}/COD medians are 1.2 and 0.9, respectively.

- temperature – optimum range is 20°C–40°C. An increase in temperature above this range accelerates the decomposition of hydrogen peroxide into oxygen and water [13,24].
- reaction time-depends on the parameters. It can range from several minutes to several hours.

In addition to the parameters mentioned above which affect the Fenton process efficiency, Mahtab et al. [12] indicated that the mode of dosing reagents produces a significant effect on the process efficiency and the amount of the resulting sludge. The experiment was carried out in three different stages at pre-set pH 3.0 for 45 min reaction time. Stage I involved single reagent dosing, stage II employed two-step reagent dosing, and in stage III three-step reagent dosing was used. The authors found that the best results (52% COD removal and 40 mL sludge production) were obtained for two-step dosing. Lower sludge production reduces secondary environmental pollution while low reagent dosing makes the process cost-effective. Gawdzik et al. [25] also reported improved efficiency of the Fenton process with sequential dosing. Studies were conducted with initial pH4 for different Fe^{2+} catalyst doses at 20°C ± 1°C and 1:10 Fe^{2+}/H_2O_2 weight ratio. The whole Fe^{2+} dose was applied at the beginning of the process. The impact of H_2O_2 dosing was examined for different dosing modes, using various doses and/or dosing times. The investigations showed that oxidant sequencing at a fixed catalyst dose results in a significant improvement in TOC (32%), COD (14%) and UVA(254) absorbance reduction in treated leachate samples when compared with the results for the reference sample.

Electro-Fenton (EF), photo-Fenton (PF) or photoelectro-Fenton (PEF) processes have become widely applied. The results reported by Crispim et al. [26] demonstrated the best organic matter removal efficiencies in terms of COD (66%, 68% and 89%) were achieved with energy consumption of only 19.41, 17.61 and 17.59 kWh·kg^{-1} COD for EF, PEF-UVA and PEF-UVC, respectively. The 4-h long process took place at 90 mA·cm^{-2}. Additionally, the authors showed that in such leachate treatment, organic and inorganic by-products, acetic and formic acids, and also NO_2^-, NO_3^- and NH_4^+ were produced. Hermosilla et al. [27] pointed out that the use of the photo-Fenton method required 32 times lower iron dose and produced 25 times less sludge volume, while COD removal effects remained the same as in the Fenton process.

Advance oxidation processes based on hydroxyl radicals ($^{\bullet}OH$) (e.g., ozonation and catalyzed ozone oxidations, Fenton and Fenton-like oxidations) and sulphate radicals ($SO_4^{\bullet}$) (e.g., activated and catalyzed persulfate oxidations) have become less satisfactory with a growing demand for increasingly efficient landfill leachate treatment. Consequently, to create a synergistic effect, they are combined with biological or physical methods [28]. Mrabet et al. [29] applied a sequence of two processes to treat landfill leachate (the city of Fez, Morocco). The optimised Fenton process (pH = 3.0, Fe^{2+} 2,000 and H_2O_2 2,500 mg·L^{-1}, 60 min process time) was followed by adsorption on bentonite (dose 3 g·L^{-1}, pH = 5, time 5 h), achieving complete COD removal and 98% color removal. Combination of the two processes gave 27% better COD removal and less than 2% better color removal. Equally satisfactory results were achieved using oxygen purification, followed by the Fenton process (Fe^{2+} 8,000 and H_2O_2 122,000 mg·L^{-1}) [11]. Santos et al. [30] noted that the use of the solar photo- Fenton-like method made it possible to eliminate coagulation–flocculation, while the resulting leachate showed improved biodegradability. According to Liu et al. [31], the peroxi-coagulation (PC) process with iron anode and modified graphite felt cathode is more cost-effective compared with the electro-Fenton (EF) and electrocoagulation (EC) processes. That happens due to the combined effect of $^{\bullet}OH$ oxidation and iron hydroxide coagulation. After the PC process, the concentrations of the examined heavy metals in the treated leachate fell below the specified emission limits. Consequently, according to [31], the preferred method for heavy metal removal was PC > EC > EF.

The complex character and instability of leachate make it necessary to develop models and use management tools for optimisation. That is especially required for hybrid treatment processes [32].

The results reported above clearly indicate that the Fenton process is highly effective for the removal of contaminants. However, every time it is necessary to carry out laboratory-scale tests to determine the optimum doses of H_2O_2 and Fe^{2+}, H_2O_2/Fe^{2+} ratios, pH and the process time. The purpose of this study was to determine second-order reaction rate constants for a new model of the kinetics of changes in COD values in leachate treated with Fenton's reagent.

2. Materials and methods

Leachate sampling, its storage and chemical composition examination were performed in accordance with the binding standard PN-ISO 5667-10:2021-11. Leachate samples (pH 7.975, COD 1,742 mg·O_2·L^{-1}, color 2,442 mg·Pt·L^{-1}, UVA(254) = 3.435) were collected from the landfill site in Janczyce, which is part of the Municipal Waste Disposal Plant in Janczyce. The facility, which has been in operation since 2003, serves a population of around 150,000. It is estimated that almost 300 kg of waste per inhabitant per year is generated in the region. At the landfill (3.64 ha), mechanically processed mixed municipal waste, sorting residues and other non-recoverable waste are deposited. On average, more than 6,600 m^3 of leachate is generated a year due to the landfill operation.

Laboratory tests on the pre-treated landfill leachate were carried out on 0.2 L leachate samples. The selected sample volume allowed the analysis of all the parameters. In the laboratory tests pure reagents were used for analysis, namely $FeSO_4{\cdot}7H_2O$ (p.a., producer chemPUR, Piekary Śląskie, Poland, applied as a 5% solution and converted to Fe^{2+} dose) and 30% H_2O_2 (p.a., producer chemPUR), and also concentrated H_2SO_4 (p.a., producer chemPUR, 98%) and KOH (p.a., producer chemPUR, 5% concentration) for pH correction.

In the partially optimised Fenton process (with Fe^{2+}/H_2O_2 weight ratio as in Table 3, and oxidation times of, respectively: 60, 90 and 120 min), the kinetics of COD value changes were examined. The tests were performed at initial pH 4 (corrected with concentrated H_2SO_4), for different Fe^{2+} catalyst doses (Fe^{2+} dose: 800, 900 and 1,000 mg·L^{-1}) at temperatures of 20°C ± 1°C, 30°C ± 1°C and 40°C ± 1°C. The Fe^{2+} doses were determined based on previous studies [31]. In order to maintain the landfill leachate temperature, the process was carried out in the shaking water bath (Fig. 1) from LaboPlay SWBN series. The stirring speed in the reaction was 50 rpm. After a pre-set oxidation time, the samples were neutralised with 5% KOH to pH = 7.5. The leachate was then stirred for 30 min at 10 rpm and finally subjected to 30 min sedimentation. Fe^{2+} and H_2O_2 were dosed as a whole at the beginning of the process.

To perform the experiment, factorial plan was designed using STATISTICA 12 by StatSoft, Inc. (Table 4).

Before and after the treatment, the following were determined in the leachate: COD, pH, color and dissolved organic compounds (UVA(254)). All analyses were carried out in accordance with currently binding standards:

- the COD was determined using the Spectroquant® photometric method, cuvette tests were performed with Spectroquant® Nova 60 spectrophotometer from Merck (Darmstadt, Germany) after prior heating in a TR 320 thermoreactor from Merck (120 min at 148°C). The applied levels of determinability were as follows: for treated leachate 15–300 mg·L^{-1} (standard deviation of the method ±1.5 mg·L^{-1}) and for raw leachate 300–3,500 mg·L^{-1} (standard deviation ±13.9 mg·L^{-1}).
- Color was determined using UV/VIS spectrophotometer in accordance with PN-EN ISO 7887:2012. The dissolved organic compounds were determined by ultraviolet spectrophotometry (254 nm wavelength) in accordance with

Table 3
Experimental range and levels of independent process factors

Parameter	Minimum (–1)	Median (0)	Maximum (+1)
[Fe], g·L^{-1}	0.8	0.9	1.0
[H_2O_2], g·L^{-1}	6.4	7.2	8.0
Time, min.	60	90	120
Temperature, K	293	303	313

Table 4
Factorial experimental design matrix coded

Experiment design 3**(4–1) fractional factorial design, 1 block, 27 runs				
No./Parameters	[H_2O_2]	[Fe]	Time	Temperature
1.	–1	–1	–1	–1
2.	–1	–1	0	1
3.	–1	–1	1	0
4.	–1	0	–1	1
5.	–1	0	0	0
6.	–1	0	1	–1
7.	–1	1	–1	0
8.	–1	1	0	–1
9.	–1	1	1	1
10.	0	–1	–1	1
11.	0	–1	0	0
12.	0	–1	1	–1
13.	0	0	–1	0
14.	0	0	0	–1
15.	0	0	1	1
16.	0	1	–1	–1
17.	0	1	0	1
18.	0	1	1	0
19.	1	–1	–1	0
20.	1	–1	0	–1
21.	1	–1	1	1
22.	1	0	–1	–1
23.	1	0	0	1
24.	1	0	1	0
25.	1	1	–1	1
26.	1	1	0	0
27.	1	1	1	–1

Fig. 1. Test stand – shaking water bath.

PN-C-04572:1984 using Genesis 150 UV-VIS spectrophotometer from Thermo Fisher Scientific (Waltham, USA).
- pH was determined potentiometrically with the pH meter, namely Multifunction Meter CX-505 in accordance with PN-EN ISO 10523:2012.

Investigations results can be analysed based on mass balance for the periodic reactor in the form of component *A* accumulation rate, which is equal to the rate of component *A* generation. That leads to Eq. (1) in the form of:

$$\frac{dn_A}{dt} = r_A V \tag{1}$$

where n_A – number of moles of component *A*, r_A – component *A* generation rate, and *V* – active volume of the reactor.

When a constant density of the reaction mixture is assumed, molar concentration of component *A* can be introduced into Eq. (1). Molar concentration is defined as:

$$n_A = c_A V \tag{2}$$

which makes it possible to transform Eq. (1) into Eq. (3).

$$\frac{dc_A}{dt} = r_A \tag{3}$$

Consider a second-order reaction which has the following form:

$$A + B \rightarrow \text{products} \tag{4}$$

The rate of consumption of components *A* and *B* can be described with Eq. (5):

$$r_A = -kc_A c_B \tag{5}$$

In addition, constant *k* is the reaction rate constant expressed in $dm^3/(mol \cdot s)$. The use of Eq. (5) and dependence Eq. (3) leads to Eq. (6).

$$\frac{dc_A}{dt} = -kc_A c_B \tag{6}$$

It will be more convenient to carry out further analysis by applying the degree of conversion of component *A*. The stoichiometry of Eq. (4) indicates the numbers of reacted moles of components *A* and *B* are equal to each other.

$$\alpha_A = \frac{C_{A0} - C_A}{C_{A0}} \tag{7}$$

Relying on the concept of degree of conversion Eq. (7), it can be concluded that Eq. (8) is a measure of moles of component *A* that have undergone reaction:

$$C_{A0} - C_A = \alpha_A C_{A0} \tag{8}$$

where c_{A0} – initial concentration of component *A*.

Because:

$$C_{A0} - C_A = C_{B0} - C_B \tag{9}$$

Eq. (10) also holds:

$$C_{B0} - C_B = \alpha_A C_{A0} \tag{10}$$

It follows directly from the equations:

$$C_A = \left(1 - \alpha_A\right) C_{A0} \tag{11}$$

$$C_B = C_{B0} - \alpha_A C_{A0} \tag{12}$$

Constant *S* will be introduced to specify the initial composition of the reaction mixture:

$$S = \frac{C_{B0}}{C_{A0}} \tag{13}$$

Constant *S* will also make it possible to transform Eq. (12) into the following:

$$C_B = C_{A0}\left(S - \alpha_A\right) \tag{14}$$

When $C_A C_B$ in Eq. (6) are substituted with Eqs. (11) and (14), the following is obtained:

$$\frac{dC_A}{dt} = -kC_{A0}^2\left(1 - \alpha_A\right)\left(S - \alpha_A\right) \tag{15}$$

By differentiating both sides of Eq. (7) with respect to *t*, the following is obtained:

$$\frac{dC_A}{dt} = \alpha \frac{dk_A}{dt} C_{A0} \tag{16}$$

and then, using this in Eq. (15), the following is received:

$$\frac{d\alpha_A}{dt} = kC_{A0}\left(1 - \alpha_A\right)\left(S - \alpha_A\right) \tag{17}$$

which is an elementary differential equation with distributed variables. The solution of the equation has the form:

$$\int_0^{\alpha_{Ak}} \frac{d\alpha_A}{\left(1 - \alpha_A\right)\left(S - \alpha_A\right)} = \int_0^{t_k} kC_{A0} dt \tag{18}$$

The integral on the right-hand side of Eq. (18) is equal to $kC_{A0}t_k$ that is:

$$\int_0^{\alpha_{Ak}} \frac{d\alpha_A}{\left(1 - \alpha_A\right)\left(S - \alpha_A\right)} = kC_{A0}t_k \tag{19}$$

To solve the integral on the left-hand side of Eq. (19), however, it is necessary to decompose the sub-integral expression into simple fractions.

$$\frac{1}{\left(1-\alpha_A\right)\left(S-\alpha_A\right)} \equiv \frac{A}{1-\alpha_A} + \frac{B}{S-\alpha_A} \tag{20}$$

The multiplication of identity Eq. (20) by the fraction of its left-hand side, yields the following:

$$1 \equiv A\left(S-\alpha_A\right) + B\left(1-\alpha_A\right) \tag{21}$$

Since the identity must be satisfied by each α_A, by substituting $\alpha_A = 1$, it is possible to determine:

$$A = \frac{1}{S-1} \tag{22}$$

By substitution of $\alpha_A = S$ into Eq. (21), constant B is determined

$$B = \frac{1}{1-S} \tag{23}$$

The substitution of Eqs. (23) and (24) into Eq. (20) yields:

$$\frac{1}{\left(1-\alpha_A\right)\left(S-\alpha_A\right)} = \frac{1}{S-1}\left[\frac{1}{1-\alpha_A} - \frac{1}{S-\alpha_A}\right] \tag{24}$$

Thus, the integral in Eq. (19) can be represented as the difference of two elementary integrals:

$$\frac{1}{S-1}\int\left(\frac{1}{1-\alpha_A} - \frac{1}{S-\alpha_A}\right)dx \tag{25}$$

After calculating the integral described by Eq. (25), the following relation is obtained:

$$\begin{aligned}&\frac{1}{S-1}\left[-\ln\left(1-\alpha_A\right)+\ln\left(S-\alpha_A\right)\right]\Big|_0^{\alpha_{Ak}}\\ &= \frac{1}{S-1}\left[-\ln\left(1-\alpha_A\right)+\ln\left(S-\alpha_{Ak}\right)-\ln S\right]\\ &= \frac{1}{S-1}\ln\frac{S-\alpha_{Ak}}{\left(1-\alpha_{Ak}\right)S}\end{aligned} \tag{26}$$

Substituting Eq. (26) into Eq. (19), the following is obtained:

$$\frac{1}{S-1}\ln\frac{S-\alpha_{Ak}}{\left(1-\alpha_{Ak}\right)S} = kC_{A0}t_k \tag{27}$$

It is easy to show that the expression $\ln\frac{S-\alpha_{Ak}}{\left(1-\alpha_{Ak}\right)S}$ can be shown in an alternative form, because we have:

$$\ln\frac{S-\alpha_{Ak}}{\left(1-\alpha_{Ak}\right)S} \equiv \ln\frac{C_B C_{A0}}{C_A C_{B0}} \equiv \ln\frac{C_B}{SC_A} \tag{28}$$

Each of the presented identity expressions is intended to correlate the results obtained.

As regards the second-order irreversible reaction, the graph of an arbitrary expression Eq. (28) over time should be a straight line. The considerations above are true only for $S \neq 1$. Values of S for COD and color are usually different from 1.

When $S = 1$, the balance Eq. (18) takes the following form:

$$\int_0^{\alpha_{Ak}} \frac{d\alpha_{Ak}}{\left(1-\alpha_A\right)^2} = \int_0^{t_k} kC_{A0}dt \tag{29}$$

Integrating Eq. (29) leads to the following relationship:

$$\left(1-\alpha_A\right)^{-1}\Big|_0^{\alpha_{Ak}} = kC_{A0}t_k \qquad \text{further:} \tag{30}$$

$$\left(\frac{1}{1-\alpha_{Ak}} - 1\right) = kC_{A0}t_k \tag{31}$$

and, after elementary transformations:

$$\frac{\alpha_k}{1-\alpha_k} = kC_{A0}t_k \tag{32}$$

or, in an alternative form:

$$\frac{C_{A0}-C_A}{C_A} = kC_{A0}t_k \tag{33}$$

3. Results and discussion

The results obtained should be correlated in the coordinate system C_{A0}–$C_A/C_{A'}$, t; in which for $S = 1$, a straight line should be obtained.

The value of $S = 1$ may be taken as the basis for determining the constant k_2 from the UVA(254) results.

If the subscript A is assigned COD or UVA(254) or color, this notation will be consistently applied to subsequent parameters and indicators. The experimental results obtained for the pre-set input parameters are listed in Table 5.

The model equation that describes the variation in the degree of conversion α for COD can be expressed as follows:

$$\begin{aligned}\alpha_{\mathrm{COD}} &= 2.795887 + 0.068754\left[\mathrm{H_2O_2}\right] - 0.001675\left[\mathrm{H_2O_2}\right]^2\\ &\quad - 0.062782\left[\mathrm{Fe}\right] + 0.067264\left[\mathrm{Fe}\right]^2 + 0.005634t\\ &\quad - 0.000019t^2 - 0.018586T + 0.000032T^2\\ &\quad + 0.053080\left[\mathrm{H_2O_2}\right]\left[\mathrm{Fe}\right] - 0.000269\left[\mathrm{H_2O_2}\right]t\\ &\quad + 0.000070\left[\mathrm{H_2O_2}\right]T - 0.000661\left[\mathrm{Fe}\right]t\\ &\quad + 0.001296\left[\mathrm{Fe}\right]t - 0.000004t\cdot T\end{aligned} \tag{34}$$

Table 5
Real values and experimental results of the response

Experiment design 3**(4–1) fractional factorial design, 1 block, 27 runs										
Run	$[H_2O_2]$, g·L^{-1}	[Fe(II)], g·L^{-1}	Time, min.	Temp., K	$\alpha_{COD,}$ –	$\alpha_{UVA(254),}$ –	$\alpha_{Color,}$ –	COD, g·L^{-1}	UVA(254), –	Color, g·L^{-1}
1.	8.00	0.90	60	293	0.7732	0.8412	0.8477	395	0.5454	101
2.	7.20	1.00	90	313	0.8292	0.9049	0.9105	298	0.3266	59
3.	6.40	0.80	90	313	0.7828	0.8545	0.8596	378	0.4999	93
4.	7.20	1.00	60	293	0.7298	0.8053	0.8058	471	0.6688	128
5.	8.00	0.90	90	313	0.8540	0.9352	0.9393	254	0.2226	40
6.	6.40	0.80	120	303	0.8362	0.9131	0.9185	285	0.2984	54
7.	8.00	0.90	120	303	0.8898	0.9831	0.9831	192	0.0580	11
8.	6.40	0.80	60	293	0.6851	0.7492	0.7530	549	0.8616	163
9.	7.20	1.00	120	303	0.8713	0.9573	0.9600	224	0.1468	26
10.	6.40	0.90	90	303	0.7780	0.8551	0.8574	387	0.4977	94
11.	6.40	0.90	120	293	0.8312	0.9137	0.9160	294	0.2963	55
12.	8.00	1.00	60	313	0.8000	0.8532	0.8684	348	0.5042	87
13.	7.20	0.80	120	293	0.8617	0.9465	0.9493	241	0.1836	33
14.	7.20	0.80	90	303	0.8109	0.8923	0.8941	329	0.3699	70
15.	7.20	0.80	60	313	0.7334	0.8040	0.8071	464	0.6732	127
16.	8.00	1.00	90	303	0.8634	0.9352	0.9445	238	0.2226	37
17.	6.40	0.90	60	313	0.6997	0.7630	0.7680	523	0.8140	153
18.	8.00	1.00	120	293	0.8985	0.9831	0.9879	177	0.0580	8
19.	7.20	0.90	120	313	0.8756	0.9566	0.9620	217	0.1490	25
20.	7.20	0.90	90	293	0.8185	0.8929	0.8986	316	0.3678	67
21.	6.40	1.00	60	303	0.6942	0.7637	0.7653	533	0.8118	155
22.	7.20	0.90	60	303	0.7309	0.8053	0.8064	469	0.6688	128
23.	8.00	0.80	120	313	0.8942	0.9825	0.9852	184	0.0602	10
24.	8.00	0.80	90	293	0.8388	0.9238	0.9253	281	0.2616	49
25.	8.00	0.80	60	303	0.7614	0.8400	0.8406	416	0.5497	105
26.	6.40	1.00	120	313	0.8410	0.9245	0.9268	277	0.2595	48
27.	6.40	1.00	90	293	0.7821	0.8557	0.8599	380	0.4956	92

As non-significant factors occurred (Fig. 2), for further considerations the form of Eq. (34) was modified. To this end, the reduction of regressors method was applied (Table 6). The method allows the use of only statistically significant ($p < 0.05$) coefficients. The reduced second-order Eq. (35) is given below, while the statistics values are included in Table 6 and Fig. 3.

As a result, the model obtained the form:

$$\alpha_{COD} = 0.120153 + 0.019305[H_2O_2] - 0.347761[Fe] + 0.007668t - 0.000019t^2 + 0.000505T + 0.056397[H_2O_2][Fe] - 0.000282[H_2O_2]t$$

The corrected model equation that describes the variation in the degree of conversion for COD can be expressed as follows:

$$\alpha_{COD} = 0.120153 + 0.019305[H_2O_2] - 0.347761[Fe] + 0.007668t - 0.000019t^2 + 0.000505T + 0.056397[H_2O_2][Fe] - 0.000282[H_2O_2]t \quad (35)$$

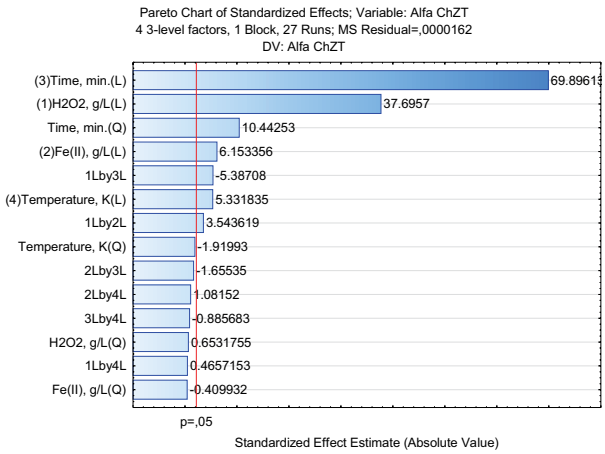

Fig. 2. Pareto chart of standardized effect estimate for α_{COD}.

Fig. 4 shows the values of the conversion degree α_{COD} as a function of oxidation time and oxidant dose for a preset temperature T = 303 K with [Fe(II)]/$[H_2O_2]$ ratio equal to 0.125. An increase in $[H_2O_2]$ concentration is accompanied

Table 6
Selected statistics values for the factors of the model equation α_{COD}

Factor	Effect estimates; Var.: Alfa ChZT; R^2 = 0.99667; Adj.: 0.99545 (correlation 1) 4 3-level factors, 1 blocks, 27 runs; MS residual = 0.0000185 DV:Alfa ChZT					
	Effect	Std. Err.	t(19)	p	–95% Cnf. Limt	+95% Cnf. Limt
Mean/Interc.	0.806103	0.000829	972.9018	0.000000	0.8043369	0.807837
(1) H_2O_2, g·L^{-1} (L)	0.071422	0.002030	35.1915	0.000000	0.0671750	0.075670
(2) Fe(II), g·L^{-1} (L)	0.011659	0.002030	5.7446	0.000016	0.0074110	0.015907
(3) Time, min(L)	0.132433	0.002030	65.2528	0.000000	0.1281850	0.136681
Time, min (Q)	0.017135	0.001758	9.7488	0.000000	0.0134560	0.020814
(4) Temperature, K (L)	0.010102	0.002030	4.9776	0.000084	0.0058540	0.014350
1L by 2L	0.009023	0.002486	3.6302	0.001782	0.003821	0.014226
1L by 3L	–0.013559	0.002486	–5.4548	0.000029	–0.018761	–0.008356

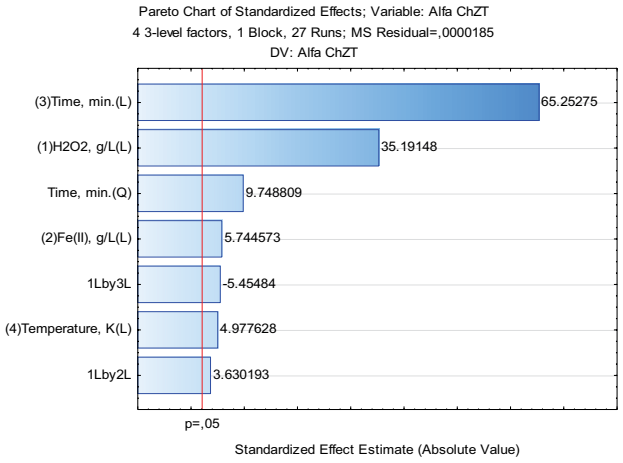

Fig. 3. Corrected Pareto chart of standardized effect estimate for α_{COD}.

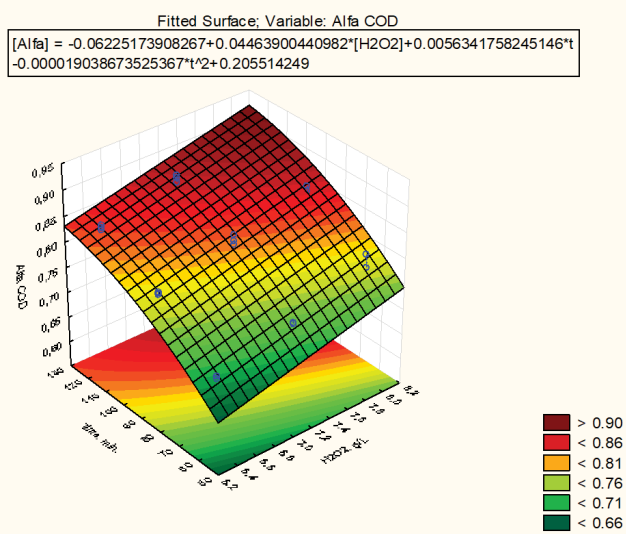

Fig. 4. The pattern of changes in the degree of conversion α_{COD} as a function of oxidation process time and the oxidant dose for the pre-set T = 303 K and [Fe(II)] concentration = 0.9 g·L^{-1}.

by increased value of the conversion degree. A similar effect was obtained due to a longer time of the process based on Fenton reagent.

The relations between the experimental data and predicted values are shown in Fig. 5. The model developed to explain the relationships holding between factors and the response showed a good congruence with the experimental values. The fit demonstrated the reduction in COD measured by the degree of conversion was described, in a satisfactory manner, with a quadratic polynomial model.

A similar approach was applied to assess the effect of leachate color removal and the UVA(254) parameter.

As a result, approximating Eqs. (36) and (37) were obtained. The model equation that describes the variation in the degree of conversion for UV can be expressed as follows:

$$\begin{aligned}\alpha_{UVA(254)} &= -0.490310 + 0.152628\left[H_2O_2\right] \\ &- 0.005255\left[H_2O_2\right]^2 + 0.075070\left[Fe\right] \\ &- 0.021020\left[Fe\right]^2 + 0.008092t - 0.000019t^2 \\ &+ 0.000540T + 0.003328\left[H_2O_2\right]\left[Fe\right] \\ &- 0.000211\left[H_2O_2\right]t - 0.000025\left[H_2O_2\right]T \\ &- 0.000192\left[Fe\right]t + 0.000154\left[Fe\right]T - 0.000001tT \end{aligned} \quad (36)$$

The model equation that describes the variation in the degree of conversion for color can be expressed by the following formula:

$$\begin{aligned}\alpha_{Color} &= -0.182356 + 0.096414\left[H_2O_2\right] - 0.003568\left[H_2O_2\right]^2 \\ &- 0.162137\left[Fe\right] + 0.007979t - 0.000020t^2 \\ &+ 0.000464T + 0.029947\left[H_2O_2\right]\left[Fe\right] \\ &- 0.000262\left[H_2O_2\right]t \end{aligned} \quad (37)$$

On the basis of the course of the function $\alpha = \alpha(C_{Fe}, C_{H2O2}, t, T)$ generated in the kinetics model for the factorial plan with three values of input quantities (–1; 0 and +1), the values of the rate constants for the second-order reaction were determined. To this end, the models Eqs. (35) and (36) & (37) were used.

Adopting model Eq. (35) makes it possible to estimate of the reaction rate constant with respect to COD. It is done by applying relation (27), which takes the following form:

$$\frac{1}{C_{A0}(S-1)}\ln\frac{S-\alpha_{Ak}}{(1-\alpha_{Ak})S}=f(t_k) \tag{38}$$

As the data can be interpolated, it is possible to generate predicted α_{COD} values also for 75 and 105 min times. Based on the above, it is possible to graphically determine the correlation between the ζ factor and the process time, where:

$$\zeta=\frac{1}{C_{A0}(S-1)}\ln\frac{S-\alpha_{Ak}}{(1-\alpha_{Ak})S} \tag{39}$$

The tangent of the slope of the regression line to the abscissa axis corresponds to the value of the rate constant k_2. (Figs. 6 and 7)

When S = 1, which happens just as the conversion degree $\alpha_{UVA(254)} = f(C_{Fe}, C_{H2O2}, t, T)$, the value of factor ζ can be expressed in a simplified form:

$$\zeta=\frac{\alpha_{Ak}}{C_{A0}(1-\alpha_{Ak})} \tag{40}$$

As it was the case for $\alpha_{COD} = f(C_{Fe}, C_{H2O2}, t, T)$, Eqs. (36) and (37) generated with STATISTICA 12 can be used to determine the slope of the regression line for ζ factor. The value of regression slope angle was crucial for the evaluation of the rate constants k_2 (Table 7).

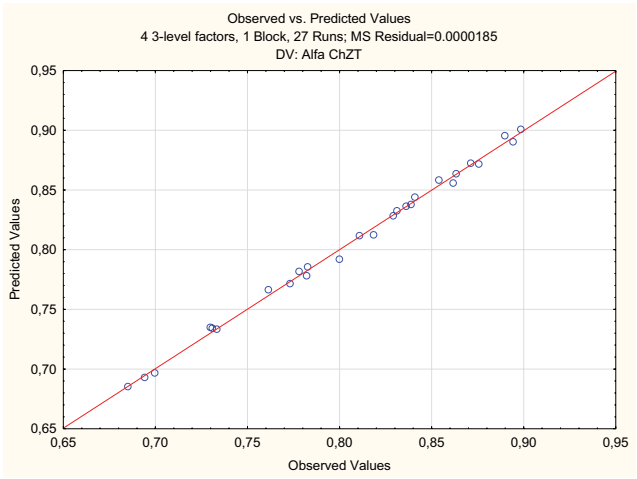

Fig. 5. Relation between experimental values and values obtained through α_{COD} prediction α_{COD}.

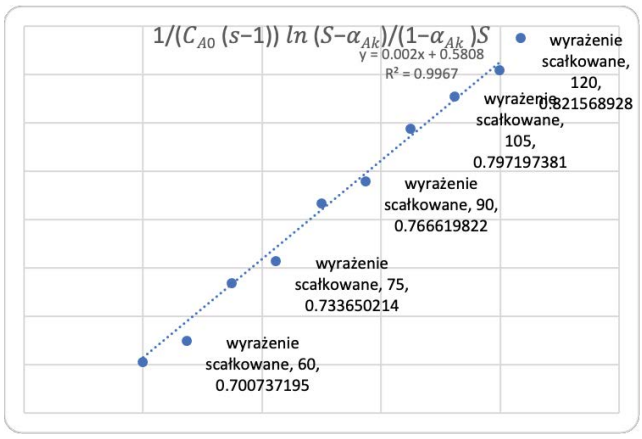

Fig. 6. Relationship between process time and factor ζ for temperature 293 K and 0.125 ratio.

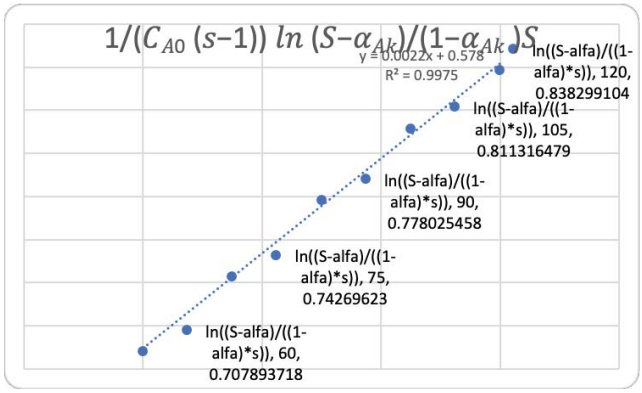

Fig. 7. Relationship between process time and factor ζ for temperature 313 K and 0.125 ratio.

Table 7
Values of rate constants k_2 in Fenton reaction determined experimentally

T = 293 K			Fe/H_2O_2	
Rate constant k_2	0.1	0.111	0.125	0.133
$k_2\alpha_{COD}$; L·g^{-1}·min^{-1}	0.0018 ± 0.0001	0.0019 ± 0.0001	0.0020 ± 0.0001	0.0021 ± 0.0001
T = 303 K			Fe/H_2O_2	
Rate constant k_2	0.1	0.111	0.125	0.133
$k_2\alpha_{COD}$; L·g^{-1}·min^{-1}	0.0018 ± 0.0001	0.0019 ± 0.0001	0.0021 ± 0.0001	0.0022 ± 0.0001
T = 313 K			Fe/H_2O_2	
Rate constant k_2	0.1	0.111	0.125	0.133
$k_2\alpha_{COD}$; L·g^{-1}·min^{-1}	0.0019 ± 0.0001	0.0020 ± 0.0001	0.0022 ± 0.0001	0.0023 ± 0.0001

In the opinion of the authors, the presented results are important and can contribute to further considerations. This paper presents only the kinetics of changes in COD of landfill leachate by the Fenton process. Due to the diversity of this environmental matrix, the above approach seems somewhat simplistic. However, comparing the results of the rate constant obtained for the three temperatures with the values taken from the literature, it can be seen that an increase in temperature only slightly increases the COD elimination efficiency of leachates. The above phenomenon can be explained by the instability of the oxidant – H_2O_2 which, according to [16,24], appears already above 300 K. Considering the above, it can be speculated that under winter conditions the Fenton process will not significantly lose its COD conversion efficiency. It was shown that the conversion degree can become a useful tool for the assessment of the oxidation reaction kinetics.

4. Conclusions

In this study, a new second-order reaction kinetics model was developed for the elimination of COD in landfill leachate treatment with Fenton reagent. It was proposed that a parameter rarely found in the literature, namely the conversion degree, should be used to determine the removal rate constant for pollution indicators selected by the authors. It was shown that the conversion degree can become a useful tool for the assessment of the oxidation reaction kinetics. Oxidation concerns landfill leachate organic pollutants in the presence of Fe(II) for different oxidant and catalyst concentrations. On the basis of the investigations, the values of the reaction rate constants k_2 were estimated. A drawback of the Fenton process is the necessity to optimise both the H_2O_2 dose, and also the appropriate Fe(II) dose required to obtain correct concentration of •OH radicals. Too high concentrations of Fe(II) ions result in generated hydroxyl radicals being scavenged. Conversely, too low catalyst content may not be powerful enough to achieve the required process progress, measured by the conversion degree value. The issues discussed above are the driving force behind the search for alternative oxidants, thus systems containing a source of Fe(VI) ions that are simpler to optimise.

References

[1] M. Franica, K. Grzeja, S. Paszula, Evaluation of quality parameters of selected composts, Arch. Waste Manage. Environ. Prot., 20 (2018) 21–32.
[2] K. Różycki, H. Ropek, Statistical analyses of bioaerosol concentration at municipal landfill site, Ecol. Chem. Eng. S, 21 (2014) 229–243.
[3] M. de Lima Elias, L.F. da Silva, L.S.M. dos Santos Lima, V.R. Amorim, M.A.G. Hinojosa, A.L.F. Menescal Conde, B. Ramalho Quintaes, J. Carbonelli Campos, Co-disposal of sludge generated during landfill leachate treatment with household solid waste, Desal. Water Treat., 159 (2019) 141–150.
[4] G.E. Blight, A.B. Fourie, J. Shamrock, C. Mbande, J.W.F. Morris, The effect of waste composition on leachate and gas quality: a study in South Africa, Waste Manage. Res., 17 (1999) 124–140.
[5] B.K. Mavakala, S. Le Faucheur, C.K. Mulaji, A. Laffite, N. Devarajan, E.M. Biey, G. Giuliani, J.-P. Otamonga, P. Kabatusuila, P.T. Mpiana, J. Poté, Leachates draining from controlled municipal solid waste landfill: detailed geochemical characterization and toxicity tests, Waste Manage., 55 (2016) 238–248.
[6] Ö. Apaydina, E. Özkan, Landfill leachate treatment with electrocoagulation: optimization by using Taguchi method, Desal. Water Treat., 173 (2020) 65–76.
[7] P. Kmet, EPA's Water Balance Method — Its Use and Limitations, Wisconsin DNR, Bureau of Solid Waste Management, Madison, P. Kemt, Ed., Water Balance Method Use and Limitations, Wisconsin Department of Natural Resources, Bureau of Solid Waste Management, 1982.
[8] M. Gomez, F. Corona, M.D. Hidalgo, Variations in the properties of leachate according to landfill age, Desal. Water Treat., 159 (2019) 24–31.
[9] L. Gao, Y. Cao, L. Wang, A review on sustainable reuse applications of Fenton sludge during wastewater treatment, Front. Environ. Sci. Eng., 16 (2022), doi: 10.1007/s11783-021-1511-6.
[10] I. el Mrabet, B. Ihnssane, H. Valdes, H. Zaitan, Optimization of Fenton process operating conditions for the treatment of the landfill leachate of Fez city (Morocco), Int. J. Environ. Sci. Technol., 19 (2022) 3323–3336.
[11] I. el Mrabet, M. Benzina, H. Valdes, H. Zaitan, Treatment of landfill leachates from Fez city (Morocco) using a sequence of aerobic and Fenton processes, Sci. Afr., 8 (2020) e00434, doi: 10.1016/j.sciaf.2020.e00434.
[12] M.S. Mahtab, I.H. Farooqi, A. Khursheed, Optimization of Fenton process for concurrent COD removal and lower sludge production: process intensification and impact of reagents dosing mode, J. Environ. Manage., 315 (2022) 115207, doi: 10.1016/j.jenvman.2022.115207.
[13] A. Babuponnusami, K. Muthukumar, A review on Fenton and improvements to the Fenton process for wastewater treatment, J. Environ. Chem. Eng., 2 (2014) 557–572.
[14] A. Aygun, T. Yilmaz, B. Nas, A. Berktay, Effect of temperature on Fenton oxidation of young landfill leachate: kinetic assessment and sludge properties, Global NEST J., 14 (2012) 487–495.
[15] I. Skoczko, Decomposition of pesticides by the Fenton method using MgO_2, Rocznik Ochrona Środowiska, 15 (2013) 1460–1473 (in Polish).
[16] K. Barbusiński, Intensification of wastewater treatment and stabilisation of excess sludge using Fenton's reagent, Politechnika Śląska, Zeszyty Naukowe nr 1603, Gliwice (2004) (in Polish).
[17] L. Dąbek, E. Ozimina, A. Picheta-Oleś, Applying the combined processes of sorption and oxidation to remove organic compounds from an aqueous environment: using the example of p-chlorophenol, Ecol. Chem. Eng. A, 19 (2012) 275–286.
[18] Y. Wu, S. Zhou, K. Zheng, X. Ye, F. Qin, Mathematical model analysis of Fenton oxidation of landfill leachate, Waste Manage., 31 (2011) 468–474.
[19] M. Ahmadian, S. Reshadat, N. Yousefi, S.H. Mirhossieni, M.R. Zare, S.R. Ghasemi, N.R. Gilan, R. Khamutian, A. Fatehizadech, Municipal leachate treatment by Fenton process: effect of some variable and kinetics, J. Environ. Public Health, 2013 (2013) 169682, doi: 10.1155/2013/169682.
[20] H. Zhang, H.J. Choi, C.-P. Huang, Optimization of Fenton process for the treatment of landfill leachate, J. Hazard. Mater., B, 125 (2005) 166–174.
[21] S.K. Singh, W.Z. Tang, Statistical analysis of optimum Fenton oxidation conditions for landfill leachate treatment, Waste Manage., 33 (2013) 81–88.
[22] S.H. Lin, C.C. Lo, Fenton process for treatment of desizing wastewater, Water Res., 31 (1997) 2050–2056.
[23] Y.W. Kang, K.-Y. Hwang, Effects of reaction conditions on the oxidation efficiency in the Fenton process, Water Res., 34 (2000) 2786–2790.
[24] K. Barbusiński, B. Pieczykolan, COD removal from landfill leachate using Fenton oxidation and coagulation, Arch. Civ. Eng. Environ., 4 (2010) 93–100.

[25] J. Gawdzik, J. Muszyńska, M. Sikorski, Effect of H_2O_2 sequential dosing in the Fenton process on leachate treatment, Desal. Water Treat., 134 (2018) 310–315.
[26] A.C. Crispim, D.M. de Araujo, C.A. Martinez-Huitle, F.L. Souza, E.V. Dos Santos, Application of electro-Fenton and photoelectro-Fenton processes for the degradation of contaminants in landfill leachate, Environ. Res., 213 (2022) 113–552.
[27] D. Hermosilla, M. Cortijo, C.P. Huang, Optimizing the treatment of landfill leachate by conventional Fenton and photo-Fenton processes, Sci. Total Environ., 407 (2009) 3473–3481.
[28] S. Li, Y. Yang, H. Zheng, Y. Zheng, T. Jing, J. Ma, J. Nan, Y. Kit Leong, J.-S. Chang, Advanced oxidation process based on hydroxyl and sulfate radicals to degrade refractory organic pollutants in landfill leachate, Chemosphere, 297 (2022) 134214, doi: 10.1016/j.chemosphere.2022.134214.
[29] I. el Mrabet, M. Benzina, H. Zaitan, Treatment of landfill leachate from Fez City by combined Fenton and adsorption processes using Moroccan bentonite clay, Desal. Water Treat., 225 (2021) 402–412.
[30] A.P.F. Santos, F. Gozzi, A.E. de Carvalho, K.R. Ferreira de Oliveira, A.R.L. Caires, R.P. Cavalcante, R.F. Cunha, D.A. da Silva, D.R. Vieira Guelfi, L. de Melo da Silva, T. Ferreira da Silva, G.A. Casagrande, S.C. de Oliveira, A. Machulek Jr., Leachate degradation using solar photo-Fenton like process: influence of coagulation–flocculation as a pre-treatment step, Sep. Purif. Technol., 289 (2022) 120712, doi: 10.1016/j.seppur.2022.120712.
[31] D. Liu, Y. Yuan, Y. Wei, H. Zhang, Y. Si, F. Zhang, Removal of refractory organics and heavy metals in landfill leachate concentrate by peroxi-coagulation process, J. Environ. Sci., 116 (2022) 43–51.
[32] C.A. dos Santos Vaz, G. Lamas Samanamud, R. Soares da Silva, A. Boscaro Franca, C.M. Finzi Quintao, A.P. Urzedo, M. Borges Silva, J.C. Bosch Neto, M. Souza Amaral, C.C.A. Loures, L.L. Rezende Naves, F.L. Naves, Modeling and optimization of hybrid leachate treatment processes and scale-up of the process: review, J. Cleaner Prod., 312 (2021) 127732, doi: 10.1016/j.jclepro.2021.127732.
[33] J. Muszyńska, Ł. Bąk, J. Górski, K. Górska, A. Sałata, J. Gawdzik, Fenton process optimization with landfill leachate in Janczyce as an example, Pol. J. Environ. Stud., 30 (2021) 3769–3775.